

AD-A165 898

SEPARATION OF ROTOR AND TEST STAND LOADS IN ROTORCRAFT  
WIND-TUNNEL TESTING(U) NATIONAL AERONAUTICS AND SPACE  
ADMINISTRATION MOFFETT FIELD CALIF P H SHINODA ET AL

1/1

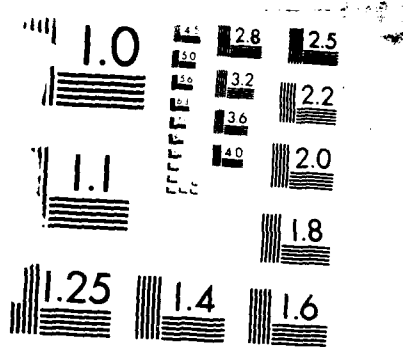
UNCLASSIFIED

1986

F/G 14/2

NL





MICROCOPY RESOLUTION TEST CHART  
NATIONAL BUREAU OF STANDARDS-1963-A

# AIAA'86

(1)

AD-A165 898

AIAA-86-0737-CP

## SEPARATION OF ROTOR AND TEST STAND LOADS IN ROTORCRAFT WIND-TUNNEL TESTING

Patrick M. Shinoda and Charles A. Smith  
NASA Ames Research Center  
Moffett Field, Calif.

DTIC FILE COPY

DTIC  
ELECTE  
MAR 27 1986  
S A

AIAA 14th Aerodynamic Testing Conference

March 5-7, 1986/West Palm Beach, Florida

This document has been approved  
for public release and sale; its  
distribution is unlimited.

024

# SEPARATION OF ROTOR AND TEST STAND LOADS IN ROTORCRAFT WIND-TUNNEL TESTING

Patrick M. Shinoda\*  
NASA Ames Research Center  
and

U.S. Army Aeroflightdynamics and Technology Activity-AVSCOM  
Moffett Field, CA 94035

and

Charles A. Smith\*  
NASA Ames Research Center, Moffett Field, CA 94035

## Abstract

Recent studies indicate that performance measurements taken in a helicopter rotor wind-tunnel test provide important information regarding the aerodynamic interaction between a helicopter rotor and a fuselage. In such tests, a large test stand (similar to a fuselage) houses the drive motor, the transmission, and other support equipment. The rotor wake can have a significant effect on both the steady-state and unsteady aerodynamic characteristics of this test stand. The magnitude of this effect is highly dependent on the test-stand shape and on the relative location between rotor and test stand. The test stand, in turn, can also affect the evolution and generation of the rotor wake and can have a significant effect on both the steady-state and dynamic rotor characteristics. Because a rotor wind-tunnel test cannot be conducted without a test stand, the true value of the isolated rotor characteristics can only be approximated from the wind tunnel data. Hence, wind-tunnel test data should be combined with analytical results for a better understanding of the isolated rotor characteristics.

## Nomenclature

A = rotor disk area,  $\pi R$ ,  $m^2$   
b = number of rotor blades  
c = rotor-blade chord, m  
 $C_{DB}$  = body wind-axis drag coefficient, positive downstream,  $D_B/q_\infty S_B$   
 $C_{LB}$  = body wind-axis lift coefficient, positive vertical toward rotor,  $L_B/q_\infty S_B$   
 $C_S$  = speed of sound, m/sec

$C_T/\sigma$  = rotor thrust coefficient divided by rotor solidity, perpendicular to tip-path-plane, positive up,  $T/\rho(\Omega R)^2 S_R$   
d = maximum body diameter, m  
 $D_B$  = body wind-axis drag, positive downstream, N  
 $D_R$  = rotor wind-axis drag, positive toward trailing edge of rotor disk, N  
h = vertical separation distance between rotor hub and body upper surface at body maximum radius, m  
L = body length, m  
 $L_B$  = body wind-axis lift, positive up toward rotor, N  
 $L_R$  = rotor wind-axis lift, positive up, N  
 $(L/D)_R$  = rotor lift-to-drag ratio,  $L_R/(P/V_\infty - PF)$   
 $M_{TIP}$  = rotor tip Mach number,  $\Omega R/C_S$   
P = rotor shaft power, Torque  $\times \Omega$ , W  
PF = rotor propulsive force,  $(-D_R)$ , N  
 $q_\infty$  = free-stream dynamic pressure, kPa  
R = rotor radius, m  
 $S_B$  = body maximum cross-sectional area,  $\pi d^2/4$ ,  $m^2$   
 $S_R$  = rotor blade area,  $bcR$ ,  $m^2$   
T = rotor thrust, perpendicular to rotor tip-path-plane, positive up, N  
 $V_\infty$  = free-stream velocity, m/sec  
 $V_W$  = hover-induced velocity (momentum theory),  $[T/(2\rho A)]^{1/2}$ , m/sec  
X = longitudinal distance from hub moment center to body nose, measured parallel to body center line, m

\*Aerospace Engineer. Member AIAA.

This paper is declared a work of the U.S. Government and therefore is in the public domain.

tion For

GRA&I

TAB

need

location

tribution/

liability Codes

Avail and/or  
Special

list

A

$\alpha_B$	= body geometric angle of attack, deg
$\alpha_S$	= rotor shaft angle, positive aft of vertical, deg
$\alpha_{TPP}$	= rotor geometric tip-path-plane angle of attack, deg
$u$	= advance ratio, $V_\infty/QR$
$\rho$	= free-stream air density, $\text{kg/m}^3$
$\sigma$	= rotor solidity, $bc/\pi R$
$\psi$	= rotor blade azimuth position, deg
$\Omega$	= rotor rotational speed, rad/sec
$\Delta D_B$	= ( $D_B$ with the rotor present) - ( $D_B$ with the rotor hub only), N
$\Delta L_B$	= ( $L_B$ with the rotor present) - ( $L_B$ with the rotor hub only), N
$\Delta(L/D)_R$	= change in rotor efficiency including body lift and drag

### Introduction

Wind-tunnel testing of helicopter rotors requires a test-stand module (typically a body of revolution) which houses the drive motor, transmission, control system, main frame, and support equipment. The test-stand module is then supported on struts near the centerline of the wind-tunnel test section. The tunnel balance system measures the aerodynamic characteristics of the combined rotor and test stand. (Note that a sting-mount configuration may be more suitable aerodynamically for certain testing but is not feasible nor practical in some cases, particularly for full-scale testing.) A full-scale helicopter rotor test-stand module used in the Ames Research Center (ARC) 40- by 80-Foot Wind Tunnel is shown in Fig. 1. To measure quantitatively the isolated rotor steady-state aerodynamic characteristics using such a test stand, the interference effects of the test stand on the rotor and the rotor on the test stand must be first understood. Several mechanisms are responsible for these interference effects. For example, the rotor wake impinges on the test stand which results in high, unsteady loads on the test-stand body.<sup>1</sup> The presence of the body in the wake affects the evolution of the rotor wake and, thus, the performance and loads on the rotor.<sup>2</sup> In most cases, each component (rotor) not only affects the flow over another component (body), it also is affected by the presence of that component in the immediate flow environment. This strong, two-way interference is referred to as aerodynamic interaction.<sup>3</sup>

This mutual interaction is shown schematically for a single rotor full-scale wind-tunnel test in Fig. 2, which is taken from Ref. 3. The

impact of these mutual interactions is that the measurement of true isolated rotor aerodynamic characteristics are not achievable. However, it can be approached by physically measuring these interactions.

Measurements of the aerodynamic characteristics of rotors in wind tunnels have often ignored the effects of the mutual aerodynamic interference between the rotor and its test stand. Standard wind-tunnel practice is often to correct rotor performance measurements only by subtracting loads measured on the isolated test stand (i.e. without the rotor) from the loads measured with the rotor installed. This approach removes the isolated test-stand loads (i.e. body-alone loads or aerodynamic tare) but does not account for any change in test-stand loads when the rotor is installed nor the influence of the test stand on the rotor flow environment. That is, it does not include aerodynamic interference between the two components. The same aerodynamic interference occurs with a helicopter. References 3-11 report investigations where rotor/fuselage interference resulted in the overall helicopter performance (i.e. aerodynamics, vibration, etc.) being significantly affected by rotor/body interaction.

An experimental and theoretical research program on rotor/body aerodynamic interaction is being conducted at ARC. This paper presents results from that program as well as other studies that encompass some of the aerodynamic effects of the rotor on the test stand, the effects of the test stand on the rotor, steady and dynamic aerodynamic characteristics, and the significance of separation of test stand and rotor performance and loads. Based on these results, recommendations are made on how wind-tunnel rotor tests can be improved.

### Discussion of Aerodynamic Interactions

#### Interference Effects On Rotor Test Stand

There are many parameters that can influence the effect of the rotor wake on the test stand's steady-state aerodynamic characteristics. These parameters include rotor tip-path-plane orientation, rotor vertical and longitudinal positions relative to the test stand, test stand angle of attack, and body shape. Some of these parameters were examined in the small-scale rotor test reported in Ref. 9. This test was conducted in the ARC 7- by 10-Foot Wind tunnel where both rotor and body were mounted independently. A 1/6-scale teetering two-bladed rotor was mounted to the tunnel balance system. A body of revolution, representing the test-stand module, was mounted to a strut that was secured to the test-section ceiling. An internal balance measured body loads. Figure 3 is a schematic of this setup. This arrangement allowed the independent measurement of each component's aerodynamic characteristics.

Results from this test which are taken from Ref. 10 are shown in Fig. 4 where the body lift is plotted vs velocity ratio. In the figure, the body lift force is normalized by the rotor thrust,  $T$ ; the horizontal axis is the ratio of wind-tunnel air speed to the average induced velocity through the rotor which is obtained from momentum theory  $V_\infty = \sqrt{T/2\rho A}$ . Plotting the results in this format provides a method of relating the effects on the body-to-rotor performance, and a means to relate a change in body load to change in the rotor-wake geometry and strength.

There are two relevant points to be made concerning this result. First, the body lift is positive. The rotor/body interaction results in a body force towards the rotor disk for this particular configuration. (The effect of a different configuration will be shown.) Second, the data from all advance ratios (ratio of free-stream velocity to rotor rotational speed) collapse onto a single curve. Thus, the overall wake parameter,  $V_\infty/V_w$ , appears to be a unifying parameter. This is reasonable as this parameter controls the proximity of the wake to the body.

As mentioned previously, conventional full-scale aerodynamic rotor performance is normally corrected by subtracting only the measured loads on the test stand with rotor blades removed. This correction is called test-stand aerodynamic tare. This test-stand tare, therefore, does not include changes induced by the presence of the rotor. An example of this is given in Fig. 5, which compares the lift on the test stand in the presence of the rotor to the lift on the isolated test stand.<sup>9</sup> This additional body lift (which would be reported as rotor thrust when using the conventional full-scale method of determining rotor performance) is affected by advance ratio and rotor thrust and can be as much as twice the lift on the isolated body. To account for this change, independent measurement of body lift is required.

Fig. 6 makes a similar comparison for the body drag.<sup>9</sup> At low advance ratio, the effects of increasing rotor thrust reduces the actual body drag virtually to zero for this configuration. However, as advance ratio increases, this sensitivity of body drag to rotor thrust diminishes. In full-scale testing, with only a single balance system measuring test stand and rotor loads, this change in body drag with rotor thrust and advance ratio would be reported as rotor drag. Based on data from Refs. 9 and 11, rotor-induced body drag contributions can increase or decrease rotor drag. Hence, body drag should also be measured independently of rotor drag to obtain a more accurate rotor drag value.

Other body loads (i.e. pitching, yawing, and rolling moments; and side force) also change with rotor thrust and advance ratio. These can, therefore, be important in determining rotor behavior using one single set of rotor/test stand performance measurements. Hence, more accurate rotor

performance with the body present is obtained if actual body aerodynamic loads are measured independently of rotor aerodynamic characteristics.

The effect of rotor/test stand body longitudinal separation is shown in Fig. 7.<sup>10</sup> It shows by moving the body forward relative to the rotor, body lift decreases and becomes increasingly negative as  $V_\infty/V_w$  is increased. This is the opposite trend to the original rotor/body location. Part of this effect is due to the rotor hub rather than the rotor blades. Pressure data from Ref. 10 showed a blockage effect forward of the rotor hub and an acceleration of the flow downstream. When the rotor hub is moved aft relative to the body, the blockage effect is now over the widest part of the body. Conversely, the accelerated flow downstream of the hub is over the narrowest part of the body.

A second small-scale rotor test is reported in Ref. 11. This test, conducted by Bell Textron Inc. in the Vought Corporation's 7- by 10-Foot Low Speed Wind Tunnel, involved a 0.15-scale teetering two-bladed rotor and a body of revolution similar to the body used in Ref. 9. The rotor and fuselage, which are shown in Fig. 8, were mounted on separate load-measurement systems. The rotor aerodynamic characteristics were measured by a five-component balance and a strain-gaged torsional mast. The body aerodynamic loads were measured by a separate six-component balance.

To show the effect of the test stand shape, four body planforms were tested. Figure 9 shows the four different body shapes: BHR represents the baseline body; BHR2FL is body BHR with a generic helicopter nose attached; BHR2FU has the same generic helicopter nose but with a smaller rotor-to-body vertical separation distance; and BHR2FWO is identical to BHR2FL but without the stub wings on the sides that would attach to the support struts on a full-scale test stand (see Fig. 10).

The influence of these four test module shapes for rotor operation at the same rotor thrust, shaft angle, and body angle as a function of advance ratio is shown in Fig. 11. Note both the magnitude and sign of the lift can change with only slight variations in test-stand configuration. Figure 11 also shows that the influence of the rotor wake on body lift is greatest for bodies with the stub wings.

#### Interference Effects On Rotor Performance and Blade Loads

There are presently little experimental data available on body/fuselage effects on steady-state rotor performance that can be used to determine effects on rotor efficiency. Data that are available are either incomplete or do not have the resolution to measure rotor performance changes owing to body inflow effects.

There are a few theoretical analyses that deal directly with body/fuselage effects on rotor performance. Reference 2 used a combination of a modified slender-body theory with a comprehensive rotor analysis to predict body-induced aerodynamic effects on rotor performance and blade loads. An example of this is shown in Fig. 12, which compares rotor lift-to-drag vs thrust for an isolated rotor and two rotor/body longitudinal positions.<sup>2</sup> The rotor  $(L/D)_R$  or rotor efficiency is a standard method of determining rotor performance in forward flight over a range of rotor-thrust conditions at various advance ratios. This ratio is a function of rotor lift, propulsive force (negative rotor drag), rotor power, and free stream velocity such that

$$(L/D)_R = L_R / (P/V_\infty - PF)$$

where

$(L/D)_R$  = rotor lift-to-drag ratio  
 $L_R$  = rotor lift  
 $PF$  = rotor propulsive force ( $-D_R$ )  
 $P$  = rotor power  
 $V_\infty$  = free-stream velocity

This figure shows that the predicted effects of a body on rotor efficiency can have a positive or negative effect on rotor efficiency. The body and rotor used in this analytical model are similar to the models used in the tests reported in Refs. 9 and 11.

Reference 1 used a modified panel method to generate the flow field around a Lynx helicopter fuselage. This body-induced flow field at the rotor disc was included in an iterative calculation of the rotor wake, which is represented by a series of vortex rings. This calculation resulted in predicted values of rotor-blade loads and rotor performance. Examples of these predicted calculations are shown in Fig. 13. They show the effect of fuselage upwash on azimuthal variation of blade lift and torque for a Lynx helicopter at 140 knots. The mean values of these curves give the rotor performance.

The presence of a body in the rotor wake not only affects rotor steady-state aerodynamic characteristics but also rotor blade dynamics. Reference 12, which compared flight test and full-scale wind-tunnel data for an S-76 rotor system, showed that the fuselage or body had a definite effect on rotor-blade dynamic loads. In addition, the magnitude of dynamic loads were influenced by the body shape. Figures 14 and 15 present a comparison of fuselage effects on rotor-blade pushrod load (i.e. torsion at the blade root) and flatwise blade bending moment dynamic loads at the 70% span.<sup>12</sup> The top two time histories in both figures are the flight and full-scale test results with the steady values of the time history adjusted so that the harmonic portion of the load variations can be compared more directly. The bottom two time histories are theoretical

calculations; one for the rotor alone, and one including an estimate of the interferences caused by the flight test fuselage.

The full-scale wind-tunnel data had a lower peak-to-peak vibratory load as compared to the flight-test data. These differences were surmised to be due to the fact that the full-scale wind-tunnel test used the ARC Rotor Test Apparatus rather than a helicopter fuselage. It was believed that this body of revolution, shown in Fig. 1 with the S-76 rotor installed, would create a smaller inflow disturbance at the rotor disk. To determine if this was indeed the case, the flow induced at the rotor disk by both the flight vehicle and the wind-tunnel test stand was calculated. These calculations are compared in Fig. 16 in terms of angle of attack at the rotor blade induced by the respective body. The figure indicates the Rotor Test Apparatus fuselage induced a lesser angle of attack distortion than the flight-test helicopter fuselage at virtually all locations in the longitudinal plane of symmetry.

Additional results taken from Ref. 2 are shown in Figs. 17 and 18. These show predicted flapwise bending moments for a rotor with and without an ellipsoid body (Fig. 17), and a rotor with and without the Rotor Test Apparatus body (Fig. 18). These two figures, as well as Fig. 15 (using the flight test vehicle fuselage), all show that the rotor alone has a lower rotor blade flapwise bending moment as compared to the rotor with a body present.

#### Interference Effects On Rotor Performance For Full-Scale Wind Tunnel Tests

Conventional full-scale aerodynamic rotor performance is normally corrected by subtracting only the measured loads on the test stand without rotor blades. As mentioned previously, this correction is the test-stand aerodynamic tare and does not include the changes induced by the presence of the rotor. Therefore, this change becomes part of the corrected rotor performance. To provide some insight into the magnitude that this body-load change contributes to the conventional method of determining rotor performance, data were taken from small-scale wind-tunnel tests where body and rotor loads were measured separately so the change in body loads induced by the rotor could be measured.<sup>9,11</sup> The range of this body-load change that can contribute to measured rotor performance, if using the conventional method of calculating rotor performance, are shown in Fig. 19 for rotor lift and Fig. 20 for effective rotor drag. For the results of these figures, body angle of attack is 0 and rotor tip-path-plane is at -4. These figures show the range of this body-load change (the difference between body load with the rotor present and the body load with the rotor hub, but without the rotor blades) for different body configurations in percentage of rotor thrust (Fig. 19) and effective rotor drag ( $P/V_\infty - PF$ , Fig. 20), respectively, as a function

of advance ratio. Though these percentages may be relatively small separately, when combined to determine rotor efficiency (as in Fig. 21) the change in body loads owing to the rotor can and does contribute to rotor performance if determined by the conventional method. Figure 21 presents the percent change in rotor efficiency between rotor loads with and without body loads at varying thrust conditions at an advance ratio of 0.30.<sup>9,11</sup> This change in rotor efficiency again depends on test-stand body shape, rotor/body relative location, rotor-wake geometry, and test-stand body angle of attack.

#### Modification of National Aerodynamics Complex Full-Scale Rotor Test Stand

As part of the National Full-Scale Aerodynamics Complex helicopter interactional aerodynamics program, a full-scale rotor test stand has been modified to enable rotor and rotor test-stand aerodynamic characteristics to be measured separately. The modified rotor test-stand module, shown schematically Fig. 22, consists of a frame, main rotor hub, transmission, swashplate assembly, gearbox, drive motor, and an aerodynamic fairing or body. The aerodynamic fairing will have 108 surface pressure ports to measure steady-state pressure. The rotor test-stand module is mounted approximately in the center of the wind-tunnel test section on a conventional three strut system; two main struts and an adjustable tail strut to vary the test-stand module angle of attack. These struts are attached to the tunnel-balance system that will measure the aerodynamic characteristics of the combined rotor system/test-stand module. The fairing/body that encloses the rotor test-stand module will be mounted on three load cells that are attached to the main frame. Each load cell measures three components: normal, axial, and side force. Two load cells are mounted on the forward portion of the body and one on the aft portion. The body lift force and body pitching moment are measured by all three load cells. The body drag force and yaw moment are measured by the two forward load cells; the aft load cell is gimbaled so only body lift loads can be transmitted. The majority of the body side force is measured by one of the forward load cells. The other forward load cell will have a bearing to allow relief of residual side loads owing to fit and temperature expansion effects. This arrangement will enable interference effects on body aerodynamic forces and moments to be measured and subtracted from measured rotor aerodynamic characteristics with the body present which include the interference effects on the body. Nevertheless, all interference effects still will not be measured. Foremost of these is the effect of the test stand on the rotor-flow environment. Because of large-scale facility limitations (i.e., it is not possible to suspend a body from the ceiling as in the small-scale tests) therefore, to account for all interference effects properly will ultimately require a combination of measurement and analytical techniques.

The purpose of the full-scale wind-tunnel test program is to study the mutual aerodynamic interactions between the main rotor and rotor test-stand module and to establish a data base for various body/rotor configurations. The specific objectives of this test configuration are to quantify the effect of separation distance between rotor and the test-stand module on main rotor loads and performance, the effect of test-stand module body configuration on main rotor loads and performance, and the effects on the fuselage steady-state body loads and surface pressure distribution with rotor-on and rotor-off configurations.

#### Conclusions

From this review of rotor/body aerodynamic interactions, the following major points can be made regarding helicopter rotor wind-tunnel testing:

- 1) The rotor does have an effect on rotor test-stand module aerodynamic characteristics. This effect depends on body size, body shape and the relative position of test-stand module body to the rotor.
- 2) The test-stand body does have an effect on both rotor aerodynamics performance and blade loads. These effects include significant changes in dynamic rotor-blade loads. The effects on steady-state rotor aerodynamic characteristics have not yet fully been determined.
- 3) Test-stand aerodynamic characteristics should be measured independently to account for the actual load on the test stand at each test condition. This will provide information to understand better rotor wake effects on body aerodynamics and will allow this effect to be removed from rotor performance.
- 4) Analytical techniques may be the only means to determine the ideal isolated rotor performance since interference effects on the rotor cannot be totally eliminated with present known experimental techniques.

The present paper has emphasized the role of rotor/body aerodynamic interference in isolated rotor testing. The role of the aerodynamic interference in the total rotorcraft performance is equally important, and it is the subject of the full-scale test program described above.

## References

- <sup>1</sup>Wilby, P. G., Young, C. and Grant, J., "An Investigation of the Influence of Fuselage Flow Field on Rotor Loads and the Effects of Vehicle Configuration," Vertica, Vol. 3, No. 2, 1979, pp. 79-94.
- <sup>2</sup>Yamauchi, G. and Johnson, W. "Development and Application of an Analysis of Axisymmetric Body Effects on Helicopter Rotor Aerodynamics Using Modified Slender Body Theory," NASA TM-85934, July 1984.
- <sup>3</sup>Sheridan, P. F. and Smith, R. P., "Interactional Aerodynamics--A New Challenge to Helicopter Technology," Journal of the American Helicopter Society, Vol. 25, No. 1, Jan. 1980, pp. 3-21.
- <sup>4</sup>Sheridan, P. F., "Interactional Aerodynamics of the Single Rotor Helicopter Configuration," USARTL-TR-78-23-A, AD/A060389, Vol. 1, Sept. 1978.
- <sup>5</sup>Wilson, John C. and Mineck, Raymond E., "Wind Tunnel Investigation of Helicopter-Rotor Wake Effects on Three Helicopter Fuselage Models," NASA TM X-3185, March 1975.
- <sup>6</sup>Balch, D. T., "An Experimental Study of Main Rotor/Tail Rotor/Airframe Interactions in Hover," 39th Annual Forum of the American Helicopter Society, May 1983, pp. 1-14.
- <sup>7</sup>Betzina, M. D. and Shinoda, P. M., "Aerodynamic Interactions Between a 1/6-Scale Helicopter Rotor and a Body of Revolution," NASA TM-84247, June 1982.
- <sup>8</sup>Betzina, M. D., Smith, C. A., Shinoda, P. M., "Rotor/Body Aerodynamic Interactions," Vertica, Vol. 9, No. 1, 1985, pp. 64-81.
- <sup>9</sup>Shinoda, P. M., "An Experimental Investigation of the Aerodynamic Interactions Between a Helicopter Rotor and a Body of Revolution," NASA TM to be published.
- <sup>10</sup>Smith, C. A. and Betzina, M. D., "A Study of the Aerodynamic Interaction Between a Main Rotor and a Fuselage," 39th Annual Forum of the American Helicopter Society, May 1983, pp. 670-702.
- <sup>11</sup>Trept, T., "A 0.15-Scale Study of Configuration Effects on the Aerodynamic Interaction Between Main Rotor and Fuselage," NASA CR-166577, to be published.
- <sup>12</sup>Jepson, D., Moffitt, R., Hilzinger, K., and Bissell, J., "Analysis and Correlation of Test Data From an Advanced Technology Rotor System," NASA CR-3714, August 1983.



Fig. 1 Full-scale helicopter rotor test stand in Ames 40- by 80-Foot Wind Tunnel.

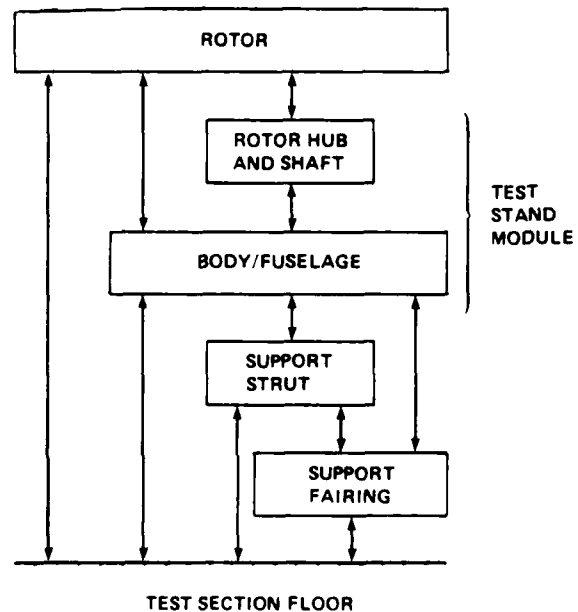


Fig. 2 Interferences on a full-scale single rotor wind tunnel test stand.

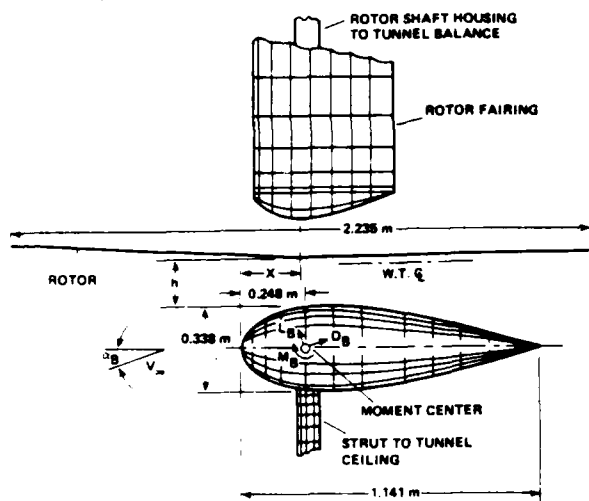


Fig. 3 Small-scale rotor and body model in Ames 7- by 10-Foot Wind Tunnel test.

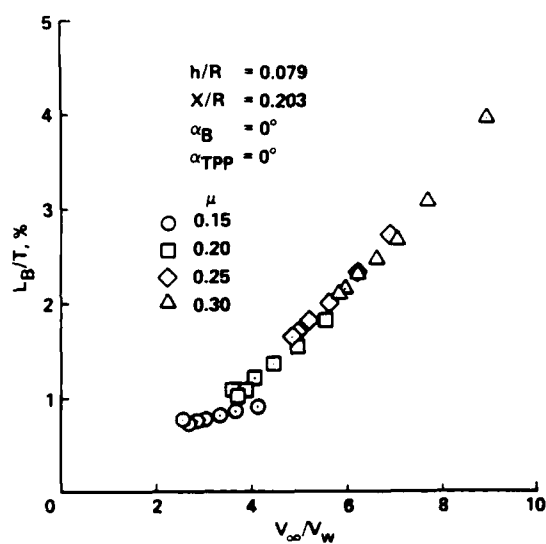


Fig. 4 Variation of body lift with velocity ratio.

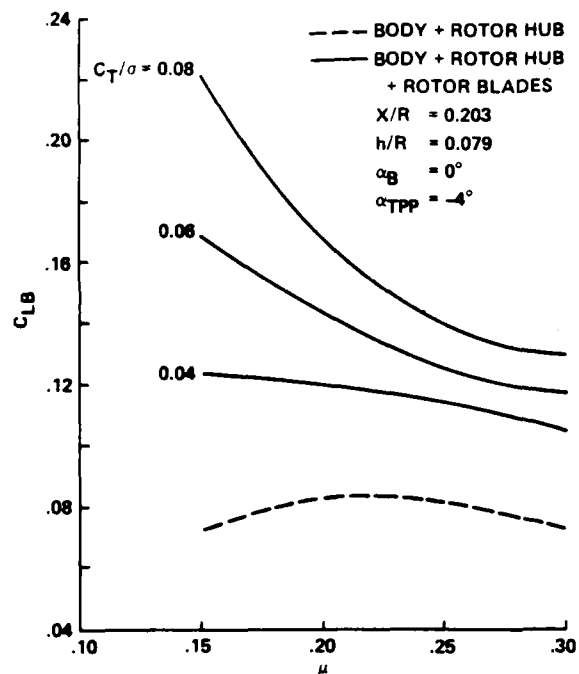


Fig. 5 Effect of a rotor on body lift.

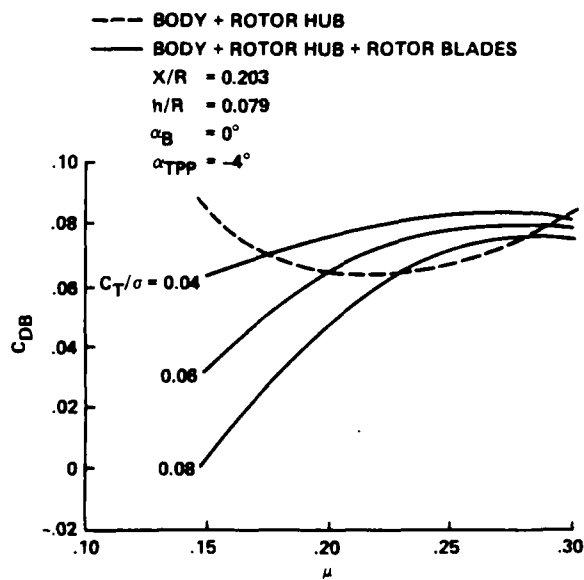


Fig. 6 Effect of a rotor on body drag.

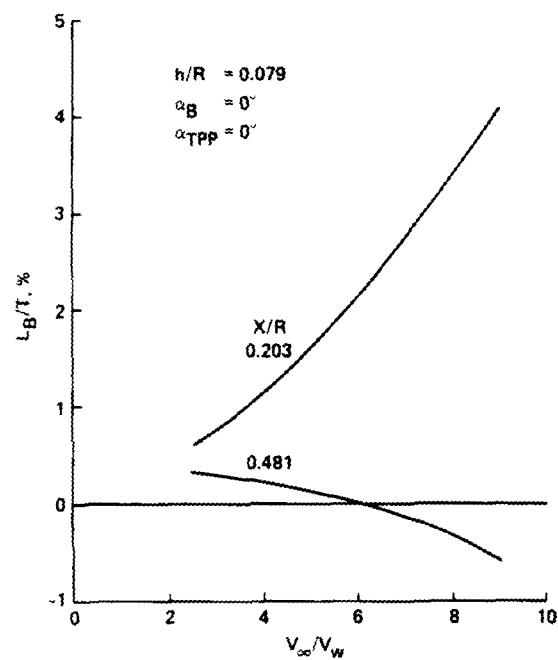


Fig. 7 Effect of rotor/body longitudinal separation on body lift.

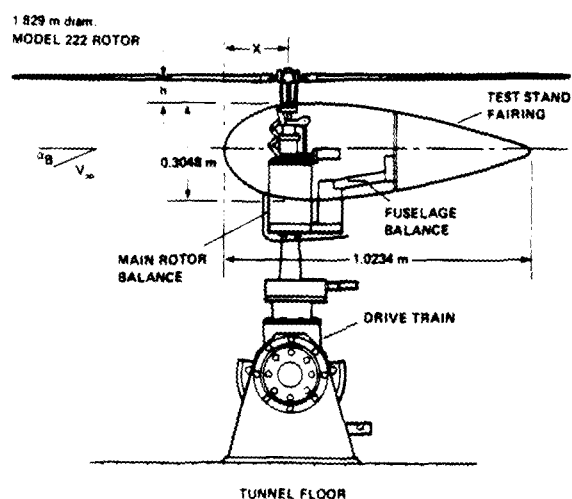


Fig. 8 Small-scale rotor and body model in Vought Corporation 7- by 10-Foot Low Speed Wind Tunnel test.

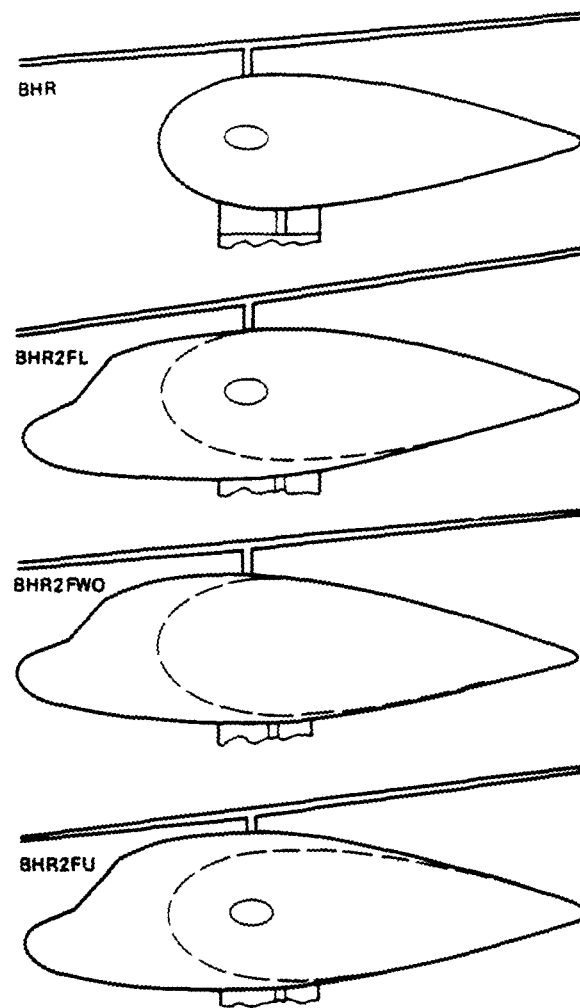


Fig. 9 Body configurations tested in Vought Corporation 7- by 10-Foot Low Speed Wind Tunnel test.



Fig. 10 Rotor test stand that will be used in full-scale rotor/body interaction test.

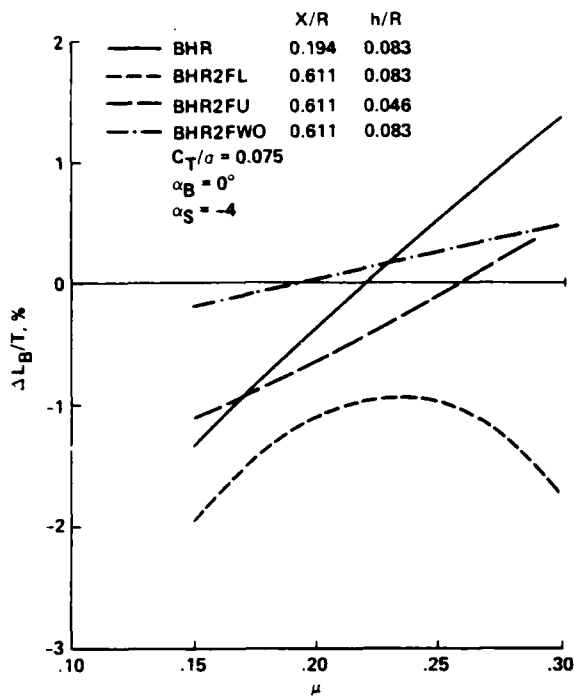


Fig. 11 Effect of a rotor on body lift for different body configurations.

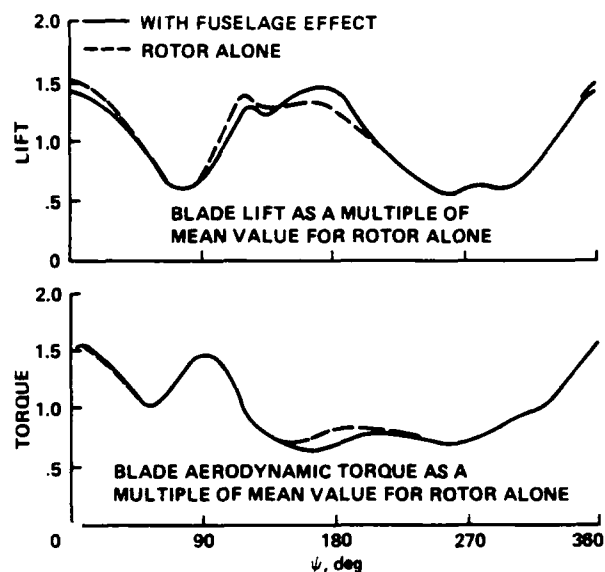


Fig. 13 Predicted effect of fuselage upwash on azimuthal variation of blade lift and torque for Lynx helicopter at 140 knots.

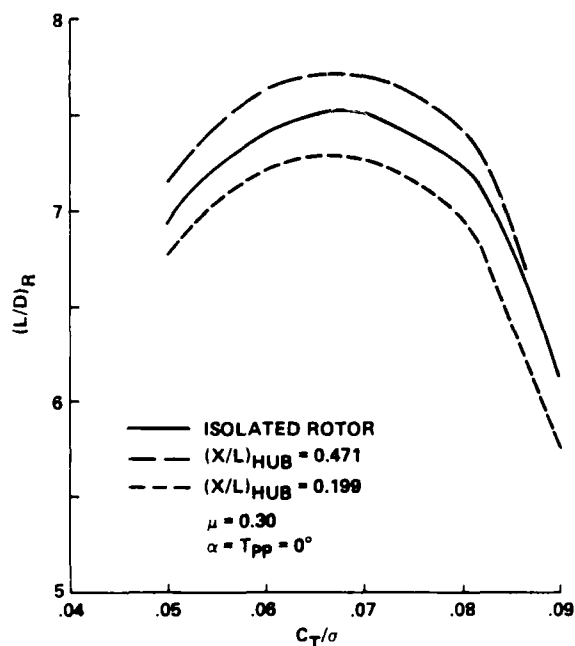


Fig. 12 Predicted effect of changing longitudinal hub position relative to a body on lift-to-drag ratio.

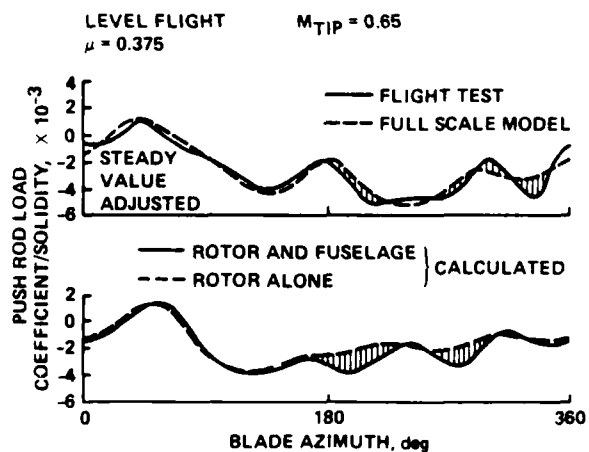


Fig. 14 Effect of fuselage on blade push rod load time history.

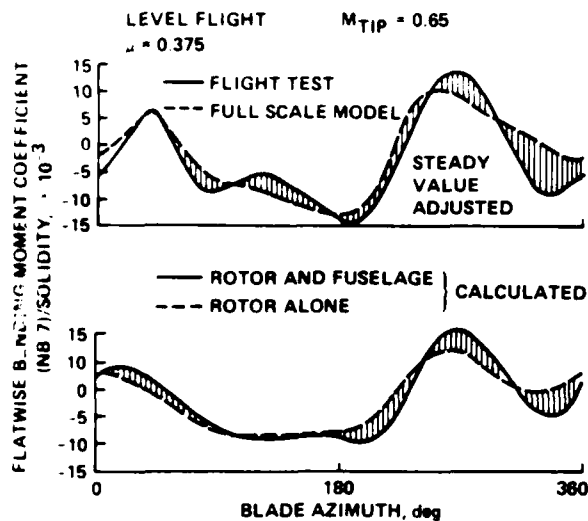


Fig. 15 Effect of fuselage on blade flatwise bending moment time history.

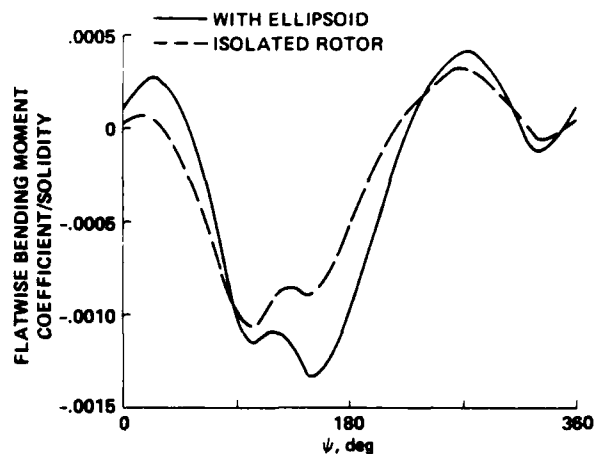


Fig. 17 Calculated time histories of flatwise bending moments at 0.6 R for a rotor at  $C_T/\sigma = 0.08$  and  $\mu = 0.4$  with an 80%-thick ellipsoid fuselage.

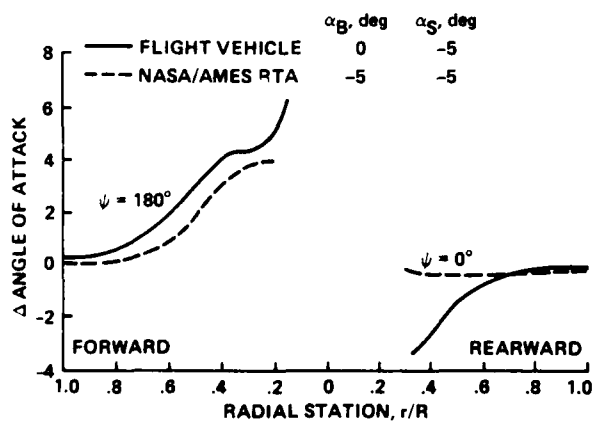


Fig. 16 Effects of fuselage-induced flow on rotor blade local angle of attack in the longitudinal plane of symmetry.

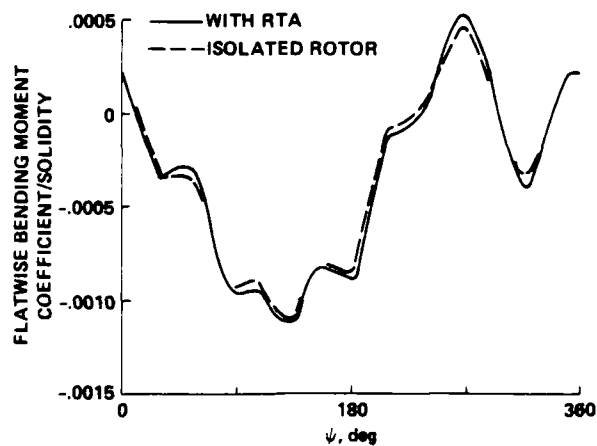


Fig. 18 Calculated time histories of flatwise bending moments at 0.7 R for a rotor at  $C_T/\sigma = 0.07$  and  $\mu = 0.5$  with the Rotor Test Apparatus fuselage.

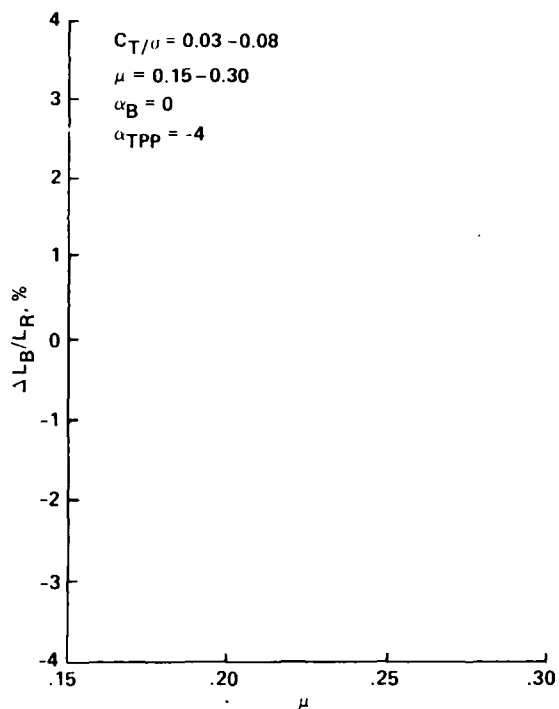


Fig. 19 Body lift contribution to rotor lift.

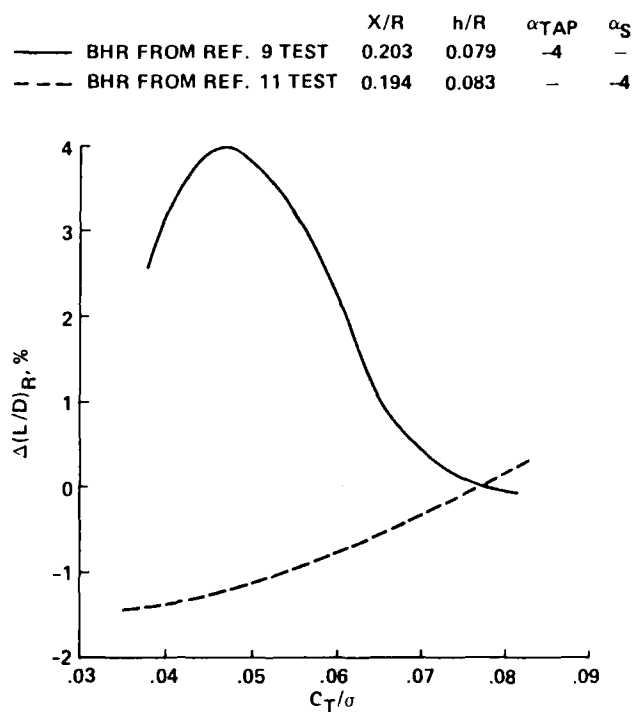


Fig. 21 Effect of body lift and drag on rotor efficiency.

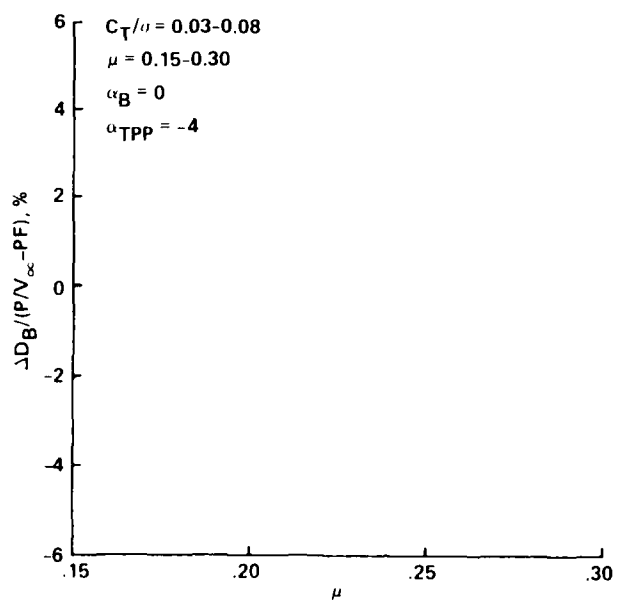


Fig. 20 Body drag contribution to effective rotor drag.

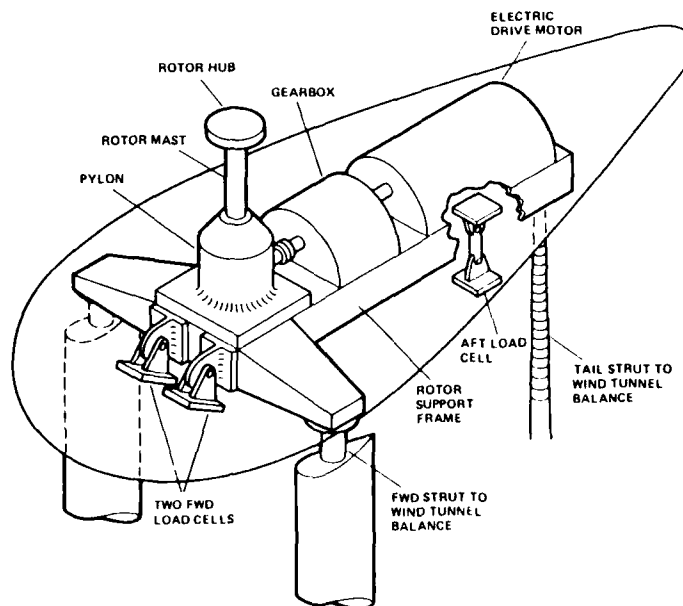


Fig. 22 Location of body load cells on the full-scale rotor test stand.

END

DTIC

4-86